

On Enhancing the Li-Ion Conductivity of Poly (ethylene oxide) based Electrolytes by suppressing the flexibility of Zeolitic Imidazolate Framework-8 via mixed ligand strategy

P. Utpalla^{1, 2}, J. Mor¹, S. K. Sharma^{1, 2*}

¹Radiochemistry Division, Bhabha Atomic Research Centre, Mumbai, India 400 085

²Homi Bhabha National Institute, Mumbai, India 400 094

Content

1. Experimental methods and characterizations

Figure S1: XRD patterns of the ZIF-7_x-8 ($x = 0, 22.1, 52.6$ and 97.2%) frameworks

Figure S2: FE-SEM images of ZIF-7_x-8 ($x = 0, 22.1, 52.6$ and 97.2%) frameworks

Figure S3: Pore sizes of ZIF-7_x-8 ($x = 0, 22.1, 52.6$ and 97.2%) frameworks determined using PALS

Figure S4: Enlarged finger print region of FTIR spectra of PEO-Li and all the QSSEs.

Figure S5: FE-SEM images of (a) ZIF-7₀-8 and (b) ZIF-7_{97.2}-8.

Figure S6. Real part (ϵ') of the complex permittivity for (a) PEO-Li (b) PEO-Li-ZIF-7₀-8 (c) PEO-Li-ZIF-7_{22.1}-8 (d) PEO-Li-ZIF-7_{52.6}-8.

Figure S7. Imaginary part (ϵ'') of the complex permittivity for (a) PEO-Li (b) PEO-Li-ZIF-7₀-8 (c) PEO-Li-ZIF-7_{22.1}-8 (d) PEO-Li-ZIF-7_{52.6}-8 (e) PEO-Li-ZIF-7_{97.2}-8.

Figure S8. dc conduction free dielectric permittivity for (a) PEO-Li (b) PEO-Li-ZIF-7₀-8 (c) PEO-Li-ZIF-7_{22.1}-8 (d) PEO-Li-ZIF-7_{52.6}-8 (e) PEO-Li-ZIF-7_{97.2}-8 QSSEs. Solid lines show the fit of experimental data using HN formalism.

Figure S9: Real part of the conductivity (σ') variation with frequency (a) PEO-Li (b) PEO-Li-ZIF-7₀-8 (c) PEO-Li-ZIF-7_{22.1}-8 (d) PEO-Li-ZIF-7_{52.6}-8 QSSEs.

Figure S10. Imaginary part of modulus, M'', variation with frequency for (a) PEO-Li (b) PEO-Li-ZIF-7₀-8 (c) PEO-Li-ZIF-7_{22.1}-8 (d) PEO-Li-ZIF-7_{52.6}-8

Figure S11. Master curve by maxima normalization technique (a) PEO-Li (b) PEO-Li-ZIF-7₀-8 (c) PEO-Li-ZIF-7_{22.1}-8 (d) PEO-Li-ZIF-7_{52.6}-8.

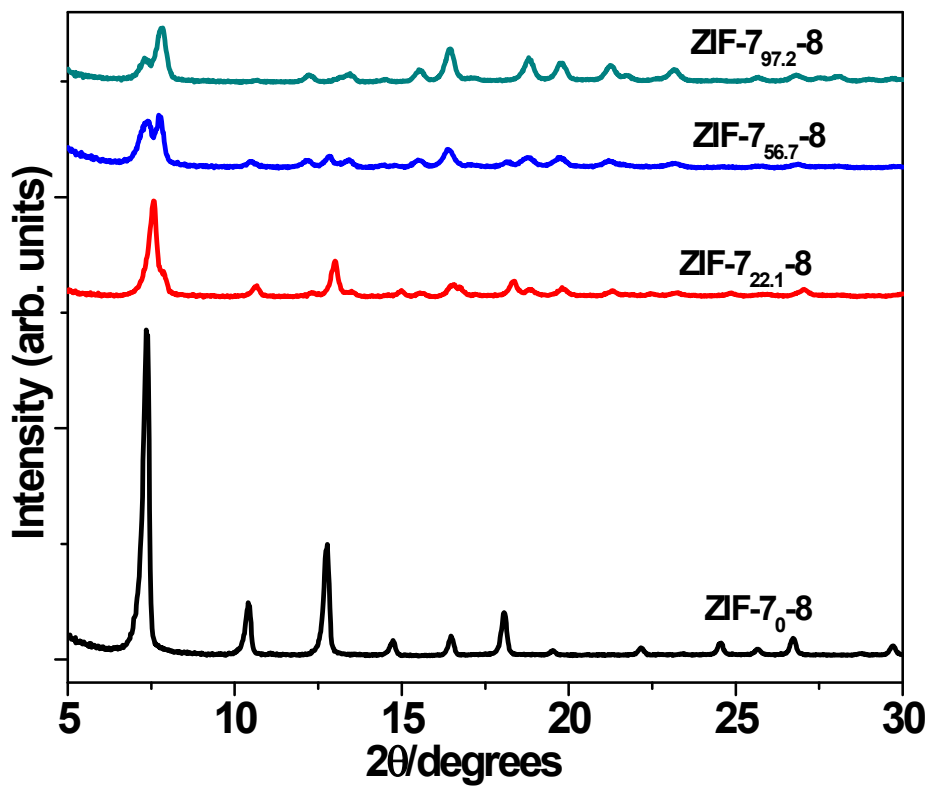


Figure S1: XRD patterns of the mixed ligand ZIF-7_x-8 ($x = 0, 22.1, 52.6$ and 97.2%) frameworks. With the increase in bIm ligand, topology of the frameworks changes from ZIF-8 to ZIF-7. The random distribution of both ligands in the framework throughout the ligand mixing ratio has been confirmed in our previous study [S1].

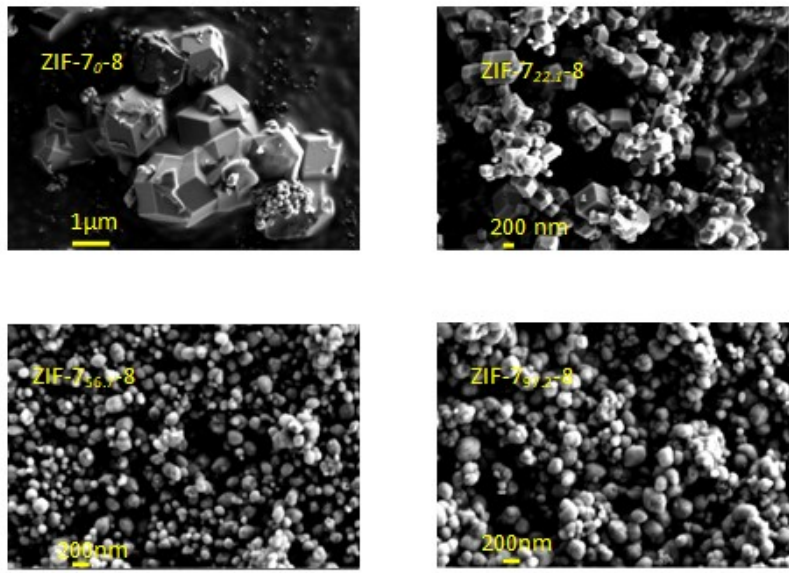


Figure S2: FE-SEM morphology of the mixed ligand ZIF- 7_x -8 ($x = 0, 22.1, 52.6$ and 97.2%) frameworks.

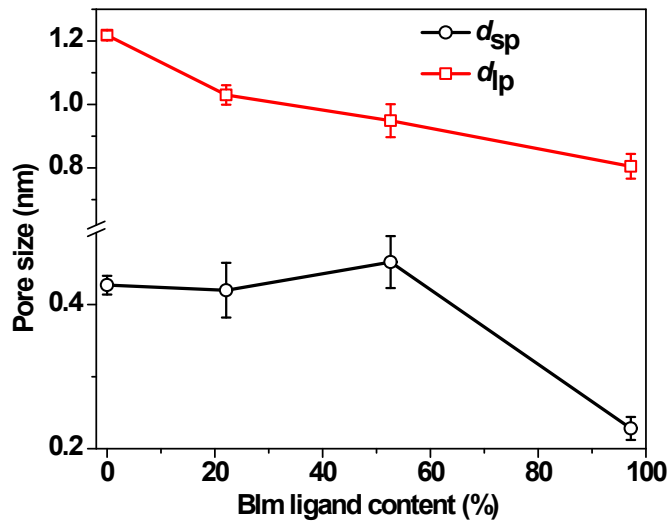


Figure S3: Pore sizes corresponding to aperture (d_{sp}) and cavity (d_{lp}) of the mixed ligand frameworks determined using PALS. The details can be found elsewhere [S1].

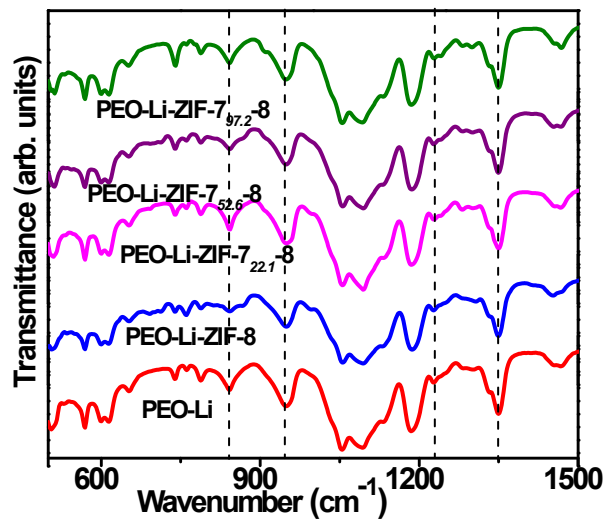


Figure S4: Enlarged finger print region of FTIR spectra of PEO-Li and all the QSSEs

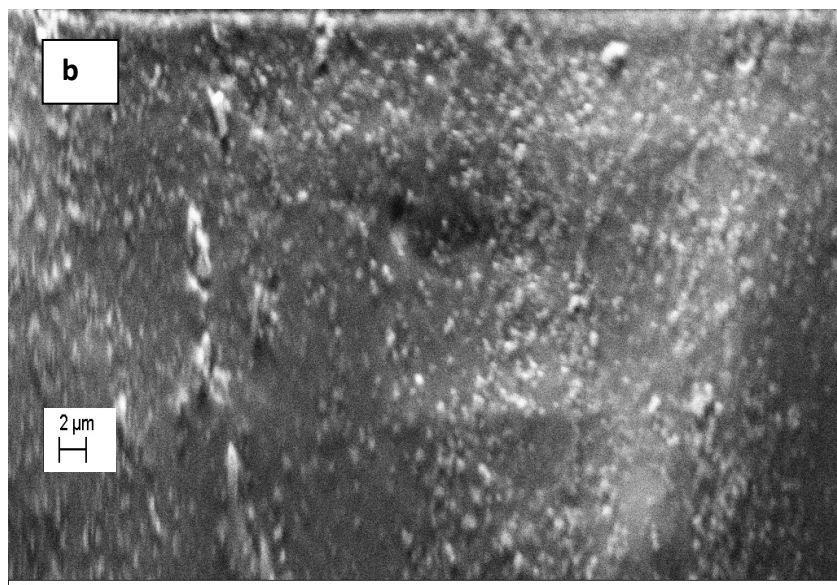
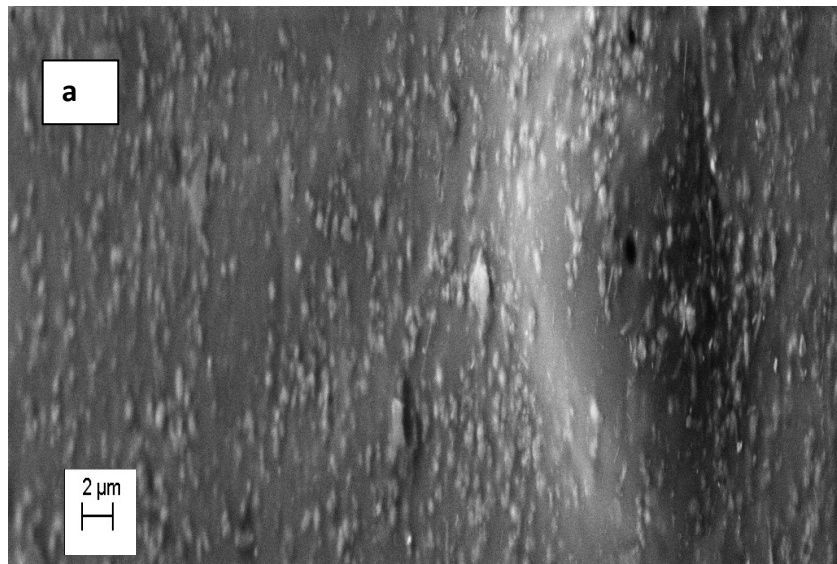


Figure S5: FE-SEM images of (a) ZIF-7₀-8 and (b) ZIF-7_{97.2}-8.

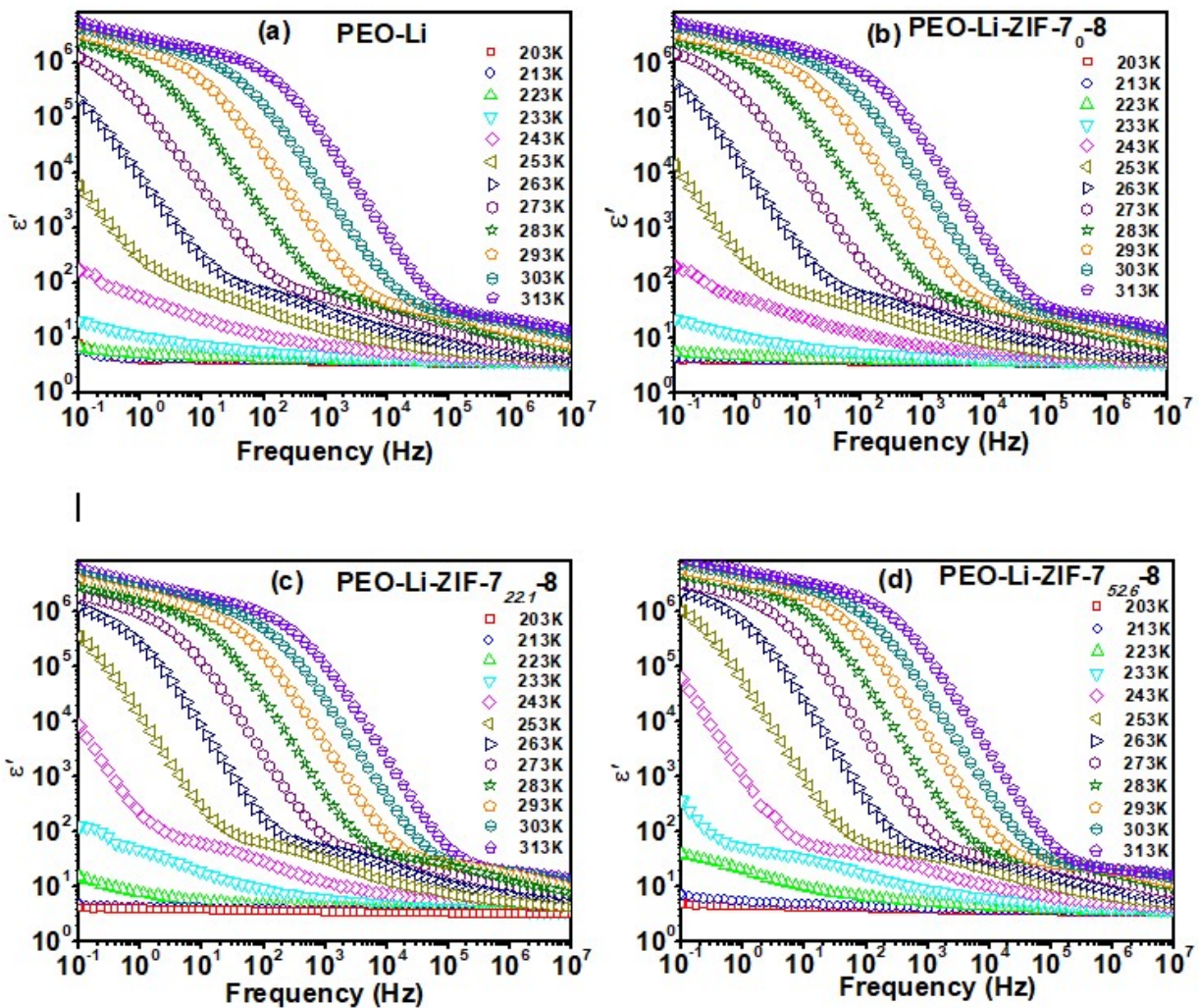


Figure S6. Real part (ϵ') of the complex permittivity for (a) PEO-Li (b) PEO-Li-ZIF-7₀-8 (c) PEO-Li-ZIF-7_{22,1}-8 (d) PEO-Li-ZIF-7_{52,6}-8.

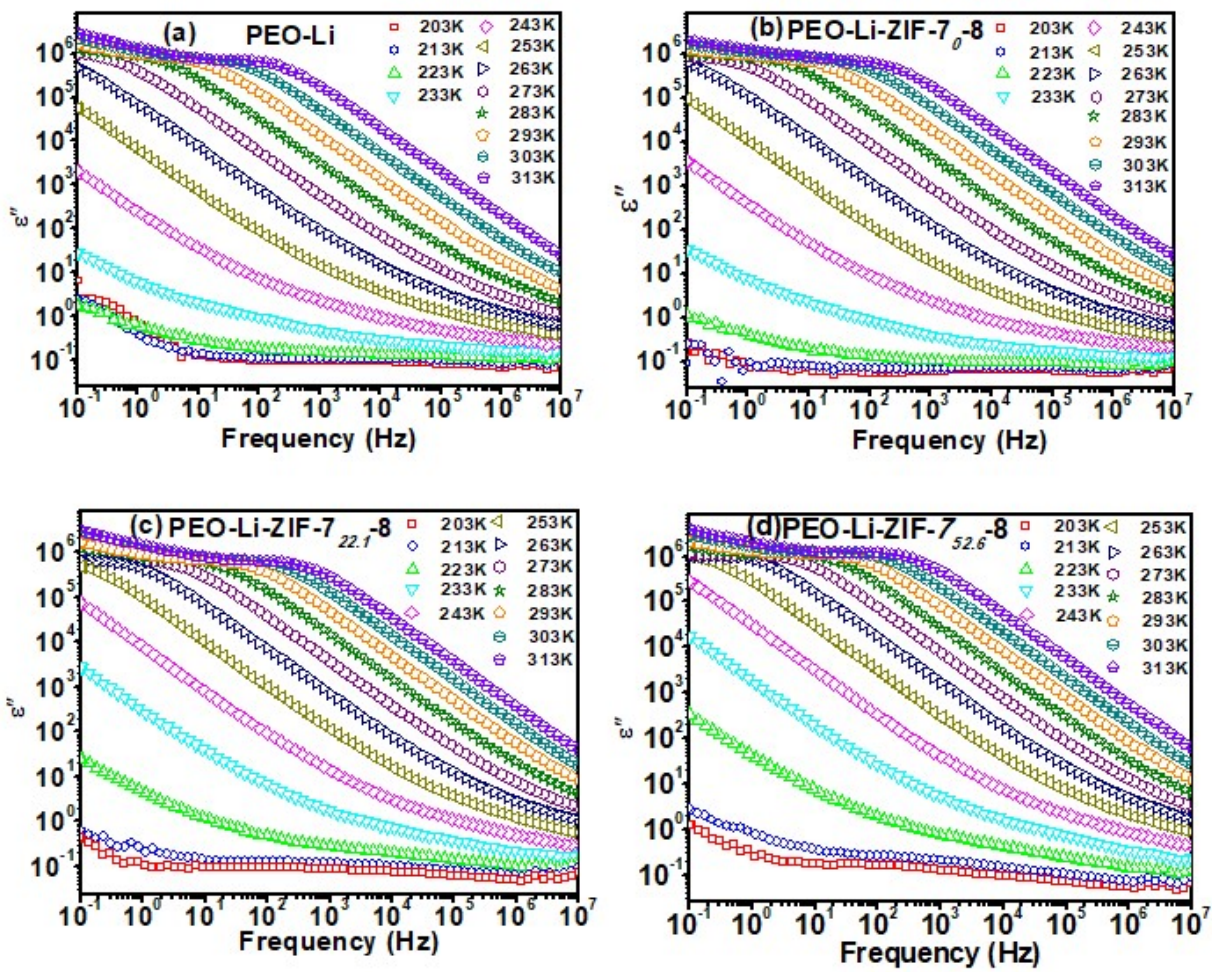


Figure S7. Imaginary part (ϵ'') of the complex permittivity for (a) PEO-Li (b) PEO-Li-ZIF-7_₀-8 (c) PEO-Li-ZIF-7_{₂₂.₁}-8 (d) PEO-Li-ZIF-7_{₅₂.₆}-8

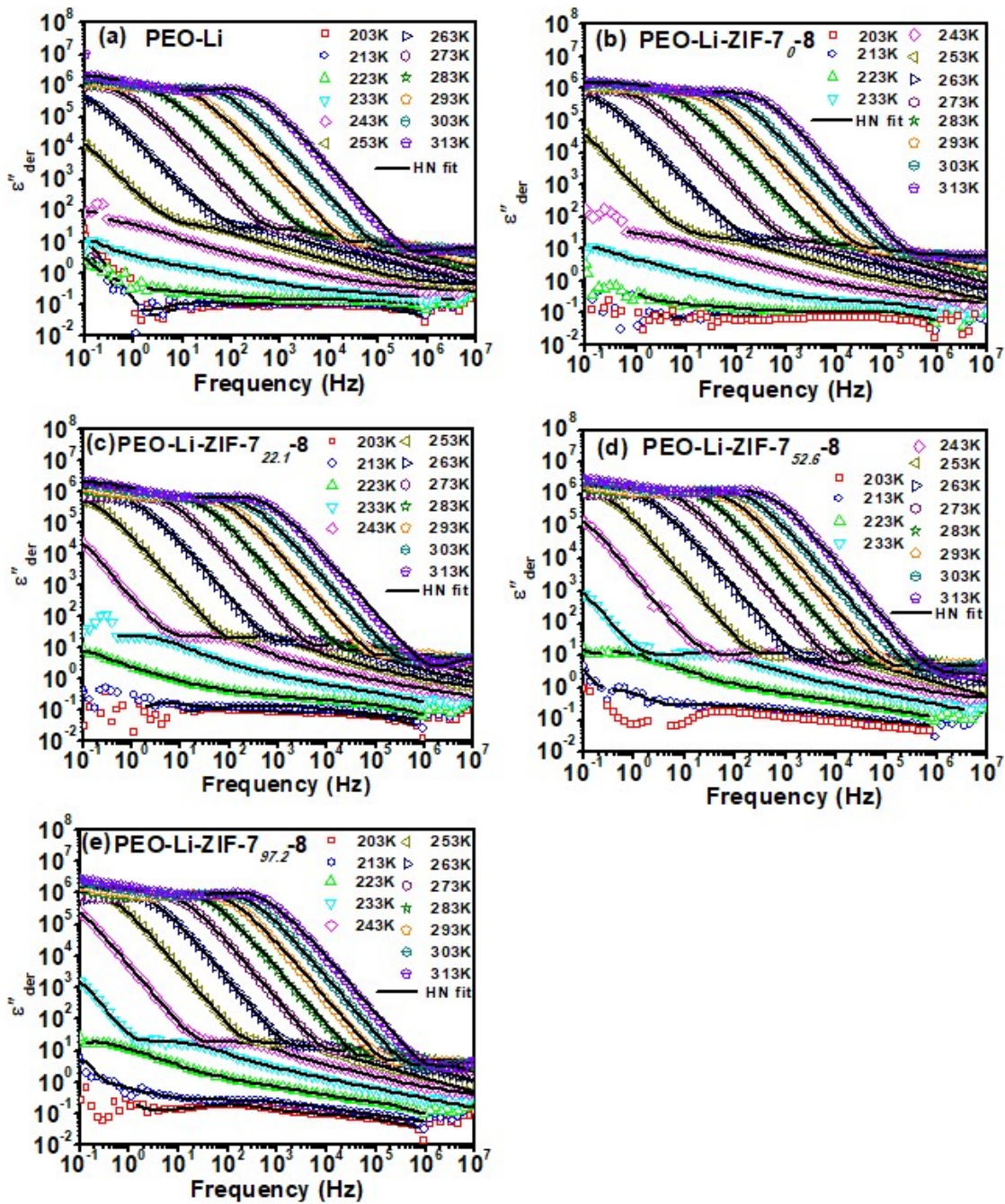


Figure S8. dc conduction free dielectric permittivity for (a) PEO-Li (b) PEO-Li-ZIF-7₀-8 (c) PEO-Li-ZIF-7_{22.1}-8 (d) PEO-Li-ZIF-7_{52.6}-8 (e) PEO-Li-ZIF-7_{97.2}-8. Solid lines show the fit of experimental data using HN formalism.

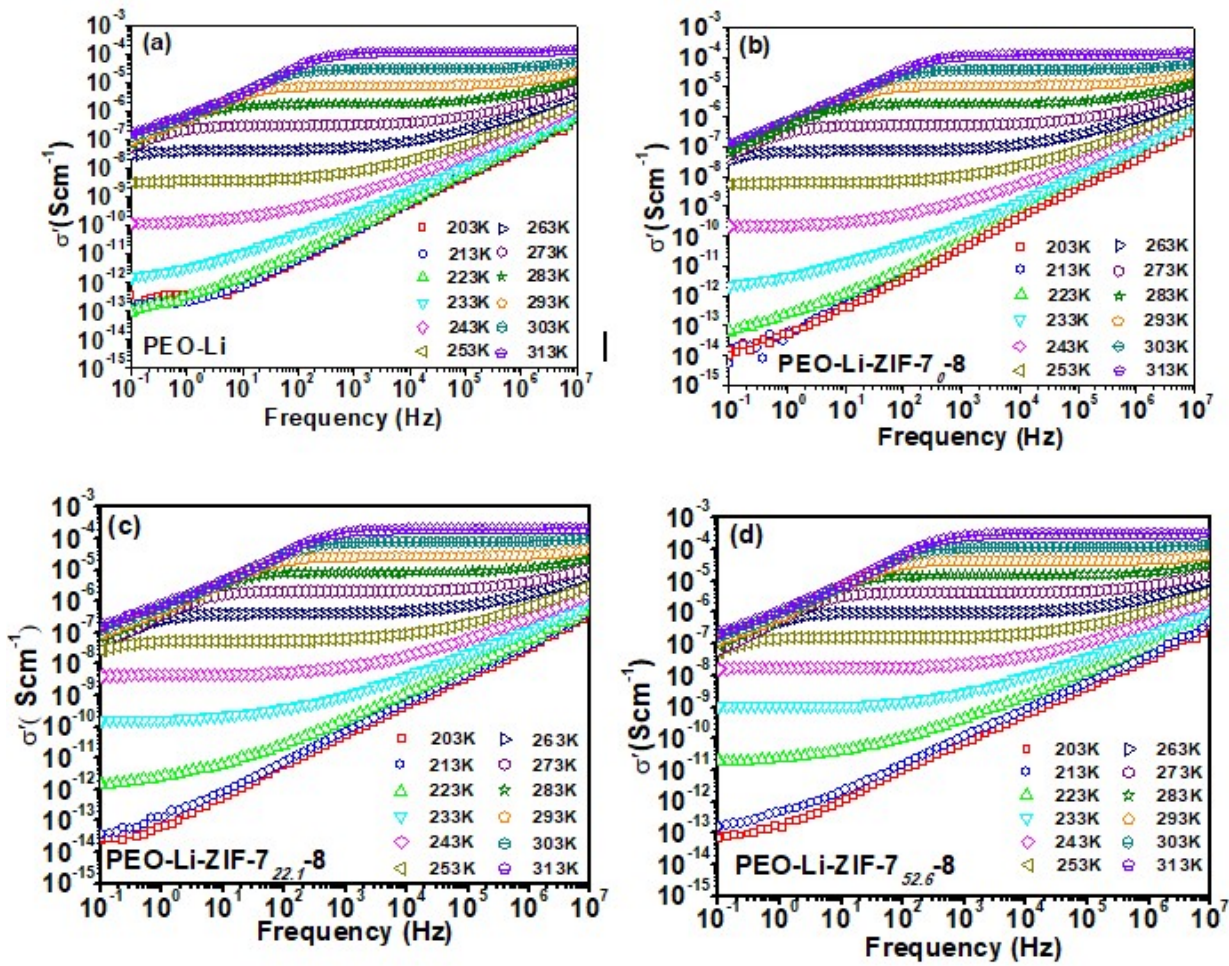


Figure S9. Real part (σ') of the complex conductivity for (a) PEO-Li (b) PEO-Li-ZIF-7_₀·₈ (c) PEO-Li-ZIF-7_{₂₂·₁}·₈ (d) PEO-Li-ZIF-7_{₅₂·₆}·₈ QSSEs.

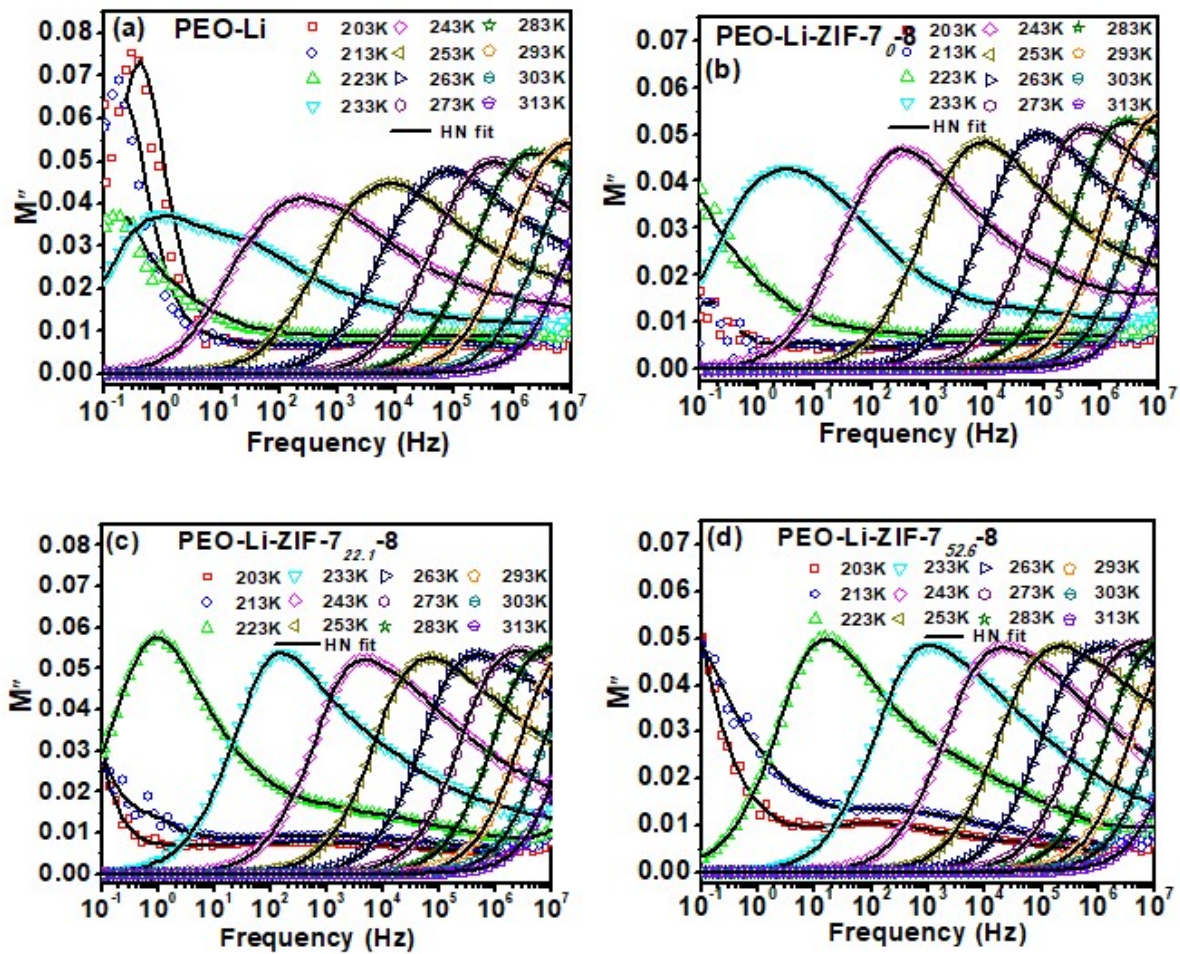


Figure S10. Imaginary part of modulus, M'' , variation with frequency for (a) PEO-Li (b) PEO-Li-ZIF-7₀-8 (c) PEO-Li-ZIF-7_{22.1}-8 (d) PEO-Li-ZIF-7_{52.6}-8

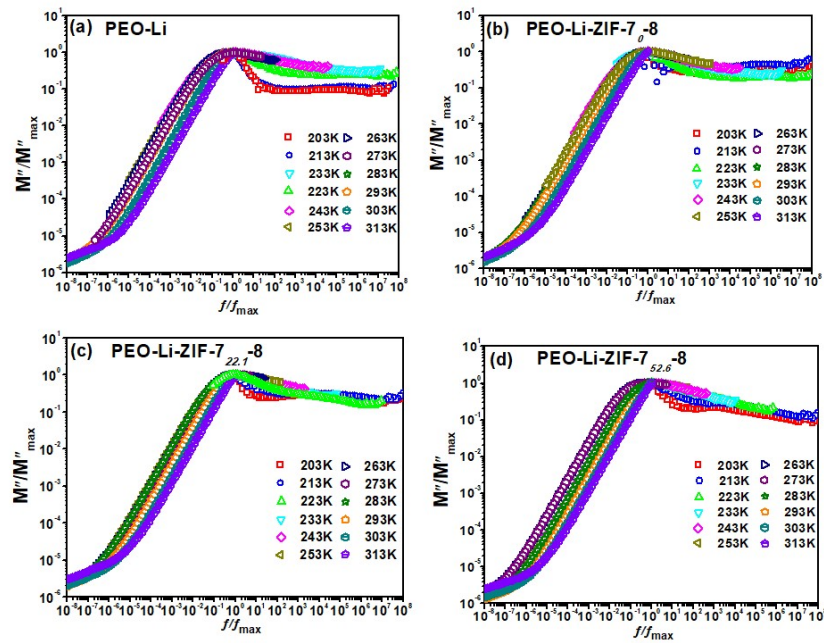


Figure S11. Master curve by maxima normalization technique (a) PEO-Li (b) PEO-Li-ZIF- 7_0 -8
(c) PEO-Li-ZIF- $7_{22.1}$ -8 (d) PEO-Li-ZIF- $7_{52.6}$ -8..